Journal of Power Sources 196 (2011) 1967–1974

Contents lists available at ScienceDirect

Journal of Power Sources

journal homepage: www.elsevier.com/locate/jpowsour

Coke formation and performance of an intermediate-temperature solid oxide fuel cell operating on dimethyl ether fuel

Chao Su, Ran Ran, Wei Wang, Zongping Shao*

State Key Laboratory of Materials-Oriented Chemical Engineering, College of Chemistry & Chemical Engineering, Nanjing University of Technology, No. 5 Xin Mofan Road, Nanjing 210009, PR China

ARTICLE INFO

Article history:
Received 17 August 2010
Accepted 1 October 2010
Available online 8 October 2010

Keywords:
Dimethyl ether
Solid oxide fuel cell
Coke formation
Anode
Reforming

ABSTRACT

Dimethyl ether (DME) as a fuel of SOFCs is investigated with great attention paid to coke formation over the Ni-YSZ anode. DME is easily decomposed to CH_4, CO and H_2 at temperatures above 700 °C, with total conversion occurring at 850 °C over the Ni-YSZ catalyst. These data suggest that the DME electro-oxidation likely proceeds via an indirect pathway. O_2-TPO analysis, laser Raman spectroscopy and SEM–EDX characterizations demonstrate coke formation over Ni-YSZ, which is obvious and become more prevalent at higher temperatures. The introduction of CO_2 in the fuel gas decreases the CH_4 selectivity and effectively suppresses coke formation above 700 °C. The suppression effect is increasingly apparent at higher temperatures. At 850 °C, the anode still maintains geometric integrity after exposure to DME–CO_2 (1:1, volume ratio) under OCV condition. With DME or DME–CO_2, the fuel cell power output is comparable to results obtained by operating with 3% water humidified hydrogen. No obvious cell degradation from the anode is observed when operating with DME–CO_2, while it is obvious with DME. The introduction of CO_2 may be a good choice to suppress the coke formation when operating on DME; however, the proper selection of operation temperature is of significant importance.

1. Introduction

With ever-diminishing oil resources and increasing environmental pollution from the inefficient burning of fossil fuels, it is crucial to find alternative and cleaner fuels and develop more efficient energy conversion techniques for a sustainable world. Recently, oxygenated hydrocarbons, such as ethers and alcohols, have been receiving increasing attention as alternative fuels [1–5]. Among them, dimethyl ether (DME) is of particular interest [6–8] because it is the simplest ether and possesses physical properties similar to those of liquefied petroleum gases, such as propane and butane. DME exists as a gas at normal conditions and is easily liquefied under 0.6 MPa of pressure at room temperature. In the liquid phase, it shows a larger volumetric and gravimetric energy density than methanol [6]. Furthermore, DME is free of sulfur, heavy metals and other impurities. Reduced NO_x, SO_x, CO, formaldehyde, particulates and non-methane hydrocarbon emissions are expected to result from replacing current fossil fuels with DME. As a secondary fuel, DME can be synthesized from primary fuels such as natural gas, coal and biomass through gasification or reforming integrated with a chemical synthesis. DME is an excellent clean energy carrier of coal and is believed to be a potential fuel for the 21 century [9]. The application of DME as an alternative fuel for gas turbines, internal combustion engines and diesel engines has been explored recently [10–12].

Fuel cells are electrochemical energy conversion devices which can generate electric power from chemical fuels with much higher efficiency and significantly lower emissions relative to conventional fire power plants [13]. Low-temperature direct DME fuel cells have been extensively investigated as a potential alternative to direct methanol fuel cells for portable application [14–19]. In such fuel cells, a polymer electrolyte is applied and the DME is directly oxidized to CO_2 and H_2O at low temperature. Compared to direct methanol fuel cells, direct DME fuel cells are less toxic and less explosive. In addition, they exhibit less fuel crossover through Nafion membrane and a higher energy density. However, DME is also less active than methanol during oxidation on conventional catalysts at normal fuel cell operational conditions and, as a result, low cell power density is obtained [20,21].

Recently, DME has also been investigated as a fuel for high-temperature solid oxide fuel cells (SOFCs) without the external reforming process [22], high power output was achieved. However, one practical problem associated with SOFC supplied directly with DME fuel is the coke formation that occurs over the nickel-based cermet anode. It is interesting that Murray et al. reported no coke formation on the anode of a SOFC operating on DME with-

* Corresponding author. Tel.: +86 25 83172256; fax: +86 25 83172256.
E-mail address: shaozp@njut.edu.cn (Z. Shao).

0378-7753/$ – see front matter © 2010 Elsevier B.V. All rights reserved.
doi:10.1016/j.jpowsour.2010.10.011

out an external reforming process at temperatures up to 700 °C [22]. However, thermodynamically, coke formation is unavoidable. Murray et al. indeed observed higher mole fractions of CO and H_2 than CH_4 at temperature lower than 700 °C, suggesting the possible formation of solid carbon. They believed that the oxygen ion current was high enough to oxidize any carbon deposited at the anode during the fuel cell operation. In principle, under open circuit conditions, no oxygen transports from the cathode to the anode, accumulation of solid carbon is then likely to happen. Especially for a long-term operation, coke formation continues to be a major concern. However, to date, the literature lacks a systematic investigation of the carbon deposition over the SOFC anode.

In this study, DME was applied as a fuel of an intermediate-temperature Ni-YSZ cermet anode-supported SOFCs. The coke formation over the Ni-YSZ cermet anode was systematically investigated. The effect of internal reforming of DME with CO_2 on the cell performance and coke formation over the anode was also studied.

2. Experimental

2.1. Synthesis and fabrication

$La_{0.8}Sr_{0.2}MnO_3$ (LSM) cathode material for SOFC was synthesized by an EDTA–citrate complexing sol–gel process [23], while NiO and $(Y_2O_3)_{0.1}(ZrO_2)_{0.9}$ (YSZ) oxide powders were purchased as commercial products (Chengdu Shudu Nano-Science Co., Ltd., China for NiO and Tosoh for YSZ). To fabricate the single cells, a tape-casting method was adopted to prepare the green anode substrates, which were fired at 1100 °C for 2 h to release the organic compounds and create sufficient mechanical strength. The electrolyte (YSZ) slurries were then spray-deposited onto the anode substrate using a modified spraying gun (BD-128, Fenghua Bida Machinery Manufacture Co. Ltd., China). The green anode-electrolyte dual layer cells were co-fired at 1400 °C for 5 h to sinter the electrolyte layer. Finally, the LSM (1000 °C calcined)-YSZ composite cathode was spray deposited onto the electrolyte surface in a round shape and fired at 1100 °C for 2 h. The effective geometric surface area is ~0.48 cm^2.

2.2. Catalytic evaluation

The thermal and catalytic decomposition of DME, CO_2 reforming of DME, and CO_2 reforming of methane was tested in a flow-through type fixed-bed quartz-tube reactor (ID: 8 mm) using Ni-YSZ cermet as the catalyst in the temperature range from 600 °C to 850 °C. After sintering at 1400 °C for 5 h (to ensure the properties similar to the anode in a real fuel cell), the NiO-YSZ anode powder was pressed into disks and milled into pellets of 40–60 mesh for the catalytic tests. Approximately 0.2 g of catalyst particles was placed into the middle of the reactor. Mixtures of DME, CO_2, He and CH_4 at the ratios of DME:CO_2:He = 10:10:80 (DME CO_2 reforming), DME:He = 10:80 (DME decomposition) and CH_4:CO_2:He = 10:10:80 (methane CO_2 reforming) were introduced from the top of the reactor. For the catalytic test, the DME and methane flow rates were fixed at 10 ml min^{-1} [STP]. The respective gas flow rate was controlled by AFC 80MD digital mass flow controllers (Qualiflow). The effluent gases from the reactor were introduced to an on-line Varian 3800 gas chromatograph (GC) for compositional analysis. The GC was equipped with Hayesep Q, Poraplot Q and 5 Å molecular sieve capillary columns, a thermal conductivity detector (TCD) for the detection of H_2, O_2, CO_2, CO and CH_4, and a flame ionization detector (FID) for analyzing DME.

2.3. Characterizations

For the carbon deposition tests, ~0.2 g Ni-YSZ particles were first placed in a flow-through type quartz-tube reactor (ID: 8 mm). The samples were then treated at various temperatures between 650 and 850 °C under pure DME or DME–CO_2 (1:1, volume ratio) for 30 min with a constant DME flow rate of 40 ml min^{-1} [STP]. After the treatment, the samples were cooled to room temperature under the protection of a helium atmosphere. Approximately 0.02 g of the powder from the treatment in DME or DME–CO_2 atmosphere was placed into a U-type quartz reactor (ID: 4 mm). A gas mixture containing 10 vol.% O_2 in Ar (10 vol.% O_2–Ar) at a flow rate of 20 ml min^{-1} [STP] was introduced to the reactor for oxygen temperature-programmed oxidization (O_2-TPO) of the deposited carbon over the catalyst. After flowing the gas at room temperature for 30 min, the reactor was heated to 900 °C at 10 °C min^{-1}. The deposited solid carbon on the Ni-YSZ surface was then progressively oxidized to CO_2. The effluent gas from the reactor was connected to a Hiden QIC-20 mass spectroscope (MS) for in situ monitoring of CO_2.

To evaluate the potential elimination of carbon deposited over the catalyst by CO_2, the catalyst was also studied by CO_2 temperature programmed reaction (CO_2-TPR) analysis after treatment in DME atmosphere. For a typical process, pure CO_2 was introduced to the reactor at the flow rate of 20 ml min^{-1} [STP]. The temperature was automatically increased at the rate of 10 °C min^{-1}, and the reaction between gaseous CO_2 and the solid carbon deposited over the catalyst proceeded. The effluent gas from the reactor was connected to an MS for on-line monitoring of the variation in CO concentration.

The laser Raman spectroscopy of the Ni-YSZ powders after the treatment at various temperatures (650, 700, 750, 800 and 850 °C) under pure DME and DME–CO_2 (1:1, volume ratio) for 30 min was conducted in an HR800 UV Raman microspectrometer (Jobin Yvon, France) using the green line of an argon laser (λ = 514.53 nm) as the excitation source.

The morphologies of cross-sections of the fuel cells were investigated by field emission scanning electron microscopy (FESEM, Hitachi S-4800) equipped with an energy dispersive X-ray analyzer (EDX) for the elemental distribution in the electrodes.

The *I–V* polarization of the cells was measured using a Keithley 2420 source meter based on 4-probe mode from 850 to 650 °C. During the measurement, 3% water humidified hydrogen, pure DME or a mixture of DME–CO_2 was fed to the anode chamber at a flow rate of 80 ml min^{-1} [STP] while ambient air was provided as the oxidant gas in the cathode chamber.

3. Results and discussion

3.1. Decomposition and CO_2 reforming of DME

One significant advantage of SOFCs compared to low-temperature fuel cells is the fuel flexibility. Methane, the simplest and most stable hydrocarbon, is thermally stable up to 850 °C because of the 410 kJ mol^{-1} C–H bond energy. By applying methane as a fuel of SOFCs, the direct electro-oxidation of methane is possible when a proper anode material is employed [24–26]. CH_3OCH_3 is the simplest oxygenated hydrocarbon in which two kinds of bonds are available, i.e., C–H and C–O. The much lower bond energy of C–O (330 kJ mol^{-1}) suggests that catalytic or thermal decomposition of DME should occur more readily than CH_4. The electro-oxidation of DME over SOFC anode is believed to proceed via an indirect pathway; it is first decomposed into CH_4, CO and H_2, which are then electro-oxidized over the anode to produce electricity [22].

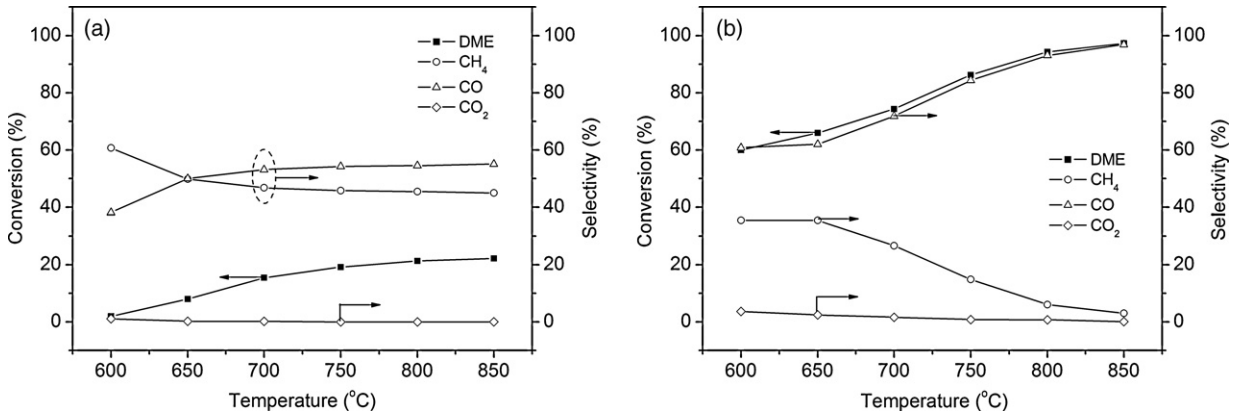

Fig. 1. The decomposition of DME without the catalyst (a) and with Ni-YSZ catalyst (b).

The decomposition behavior of DME was first tested at various temperatures with and without the presence of Ni-YSZ cermet. CO, CH_4 and H_2 are the main products for both thermal and catalytic decomposition of DME, in agreement with published observations [22]. As shown in Fig. 1(a), at 600 °C, the thermal decomposition of DME is negligible, with a DME conversion of less than 2%. In addition to CO, H_2 and CH_4, a small amount of CO_2 was also detected at 600, 650 and 700 °C. However, it was not produced at temperatures above 700 °C. The DME conversion increased steadily with temperature and reached a value of ~22% at 800 °C. This result suggests that DME was already partially decomposed before reaching the fuel cell anode, especially at temperatures greater than 750 °C. The slightly higher selectivity for CO, relative to CH_4, implies coke may also be formed during the thermal decomposition. Fig. 1(b) shows the DME conversion and selectivities for CH_4, CO and CO_2 at various temperatures with the presence of Ni-YSZ cermet. Compared to the blank run (thermal decomposition), a substantial increase in DME conversion was observed at all investigated temperatures, suggesting the catalytic effect of Ni-YSZ during DME decomposition. For example, the DME conversion was ~60% at 600 °C and ~94% at 800 °C. Therefore, the electro-oxidation of DME over a Ni-YSZ cermet anode in a conventional SOFC likely proceeds via an indirect pathway; the DME first decomposes to H_2 and CO before being electro-oxidized.

The stoichiometric decomposition of DME to CO, H_2 and CH_4 should result in 50% selectivity for both CO and CH_4. However, the actual CH_4 selectivity is substantially less than that of CO, even at 600 °C over Ni-YSZ cermet; this value is only ~3% at 850 °C. These data imply that substantial amounts of coke could be forming. This phenomenon is well understood because nickel catalyzes the cracking of hydrocarbons. The in-depth discussion about coke formation will be presented in the next section. The increase of the O/C ratio is a practical way to suppress the coke formation. CO_2 is a deep electrochemical oxidation product of DME, which has a high O-to-C ratio. In this study, CO_2 was introduced as a reforming gas for DME in order to suppress coke formation.

Fig. 2(a) shows the DME and CO_2 conversions and the selectivities for CH_4 and CO at various temperatures. Compared to the thermal decomposition of pure DME, only a slight improvement in DME conversion was observed. The CO_2 conversion was also low with a value of approximately 22% at 850 °C. These results suggest that the homogeneous gas-phase reaction between CO_2 and DME (or the decomposition products) is weak between 600 and 850 °C. Fig. 2(b) shows the DME and CO_2 conversions and the selectivities for CH_4 and CO at various temperatures after introducing Ni-YSZ as a catalyst. The CO_2 conversion reached ~58% at 600 °C and increased to ~93% at 750 °C. These data suggest that nickel anodes catalyze the reaction between CO_2 and DME or its decomposition products. Compared to the decomposition of pure DME over Ni-YSZ cermet, as shown in Fig. 1(b), an increase in DME conversion and a decrease in CH_4 selectivity at all corresponding temperatures were demonstrated by introducing CO_2. Thus, CO_2 likely reacted with both DME and its decomposition products, such as methane and solid carbon. The catalytic activity of Ni-YSZ towards the CO_2 reforming of methane (CH_4:CO_2 = 1:1) is shown in Fig. 3. By comparison, the non-catalytic and homogeneous reaction between CH_4 and CO_2 is also presented. The CH_4 and CO_2 conversions at 800 °C are both greater than 95%.

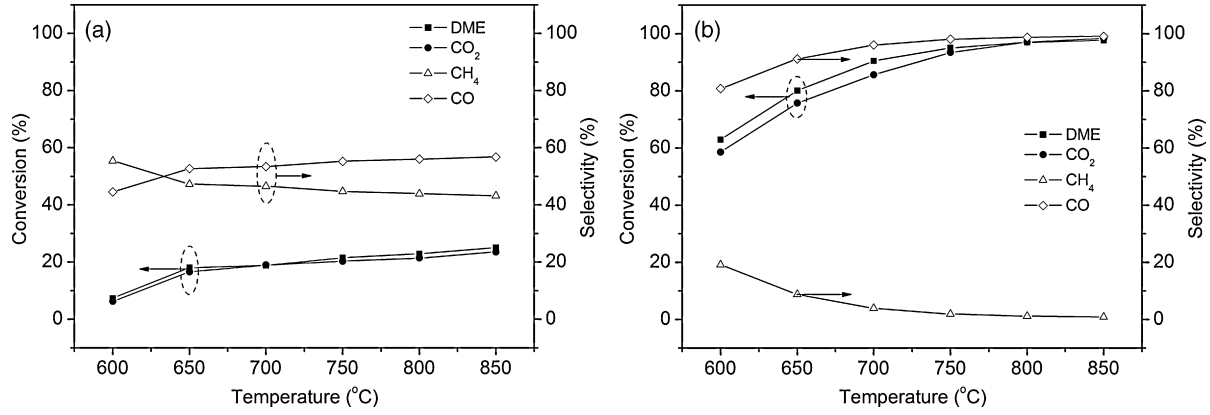

Fig. 2. The CO_2 reforming of DME (DME:CO_2 = 1:1) without the catalyst (a) and with Ni-YSZ catalyst (b).

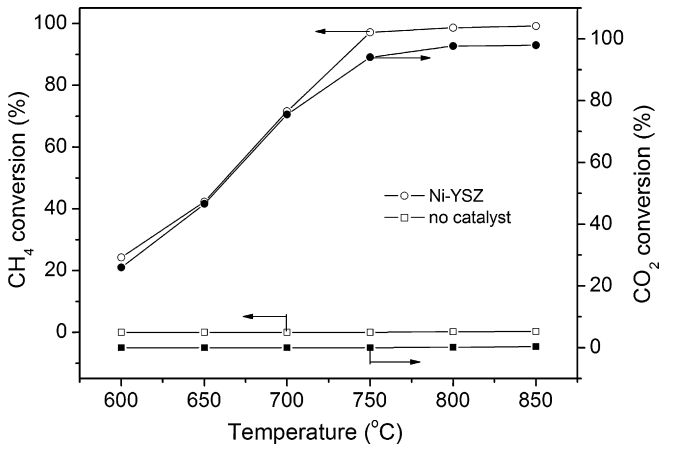

Fig. 3. The methane CO_2 reforming (CH_4:CO_2 = 1:1) with and without the Ni-YSZ catalyst.

3.2. Coke formation

In principle, SOFCs can directly operate on a wide range of fuels without the external reforming process. However, coke can easily form over conventional nickel-based cermet anodes with hydrocarbon fuels. The carbon covers the active sites and leads to a fast decay in cell performance. Furthermore, the accumulation of carbon could lead to the failure of the fuel cell by destroying the geometric integrity of the cell. Based on above catalytic tests, serious coke formation is likely occurring over the Ni-YSZ catalyst when the cell is operating on pure DME fuel.

The carbon deposition properties of the Ni-YSZ electrode when operating on DME fuel were first examined by treating the Ni-YSZ cermet anode powders in a pure DME atmosphere at various temperatures for 30 min. The as-obtained samples were then subjected to O_2-TPO analysis. Fig. 4(a) shows the O_2-TPO profiles with the CO_2 signal. Broad CO_2 peaks were observed for all samples. The CO_2 was formed from the oxidation of the solid carbon deposited on the Ni-YSZ during the programmed heating process. Coke formation over the Ni-YSZ occurred under the open circuit conditions. An increase in the peak intensity was observed at elevated temperatures, suggesting more severe coke formation. This result can be explained by the increased reaction kinetics and agrees with the decreased CH_4 selectivity, as shown in Fig. 1(b). The enhanced carbon deposition is more clearly demonstrated by the larger CO_2 peak area at higher temperature, as listed in Table 1. The average coke formation rate at 850 °C is greater than 3 times the rate at 650 °C.

Table 1
CO_2 peak area of O_2-TPO profiles of Ni-YSZ after the treatment in pure DME or DME–CO_2 at various temperatures.

Temperature (°C)	CO_2 peak area	
	DME atmosphere	DME–CO_2 atmosphere
850	8.49E−6	1.90E−7
800	4.77E−6	4.23E−7
750	3.51E−6	1.38E−6
700	2.99E−6	3.14E−6
650	2.51E−6	2.42E−6

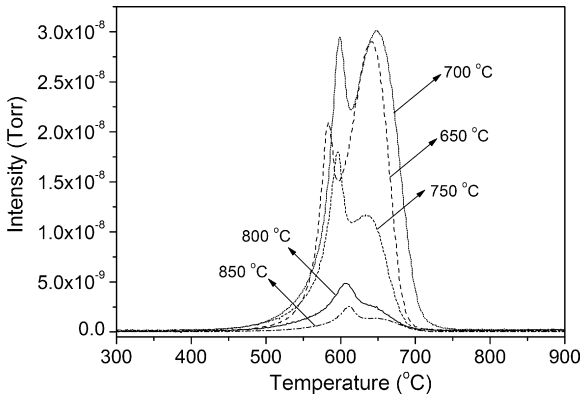

Fig. 5. O_2-TPO profiles of Ni-YSZ after treatment in DME–CO_2 (DME:CO_2 = 1:1) for 30 min at various temperatures.

It is well known that Ni-YSZ cermet anode catalyzes methane pyrolysis at elevated temperatures [27–29]. Murray demonstrated that carbon deposition at high temperatures from DME fuel is likely created via an indirect pathway by the pyrolysis of CH_4. To demonstrate the origin of the deposited carbon, Ni-YSZ was treated in CH_4 at 850 °C for 30 min; the obtained sample was studied by O_2-TPO analysis. As shown in Fig. 4(b), the CO_2 peak intensity for the sample treated in CH_4 is more than half of the value for the sample treated in DME. This result implies that the carbon deposition over the Ni-YSZ cermet when operating on DME fuel is not simply from the catalytic decomposition of CH_4. The decomposition of CH_4 may partially contribute to the carbon deposited on the Ni-YSZ cermet.

Fig. 5 shows the O_2-TPO profiles of Ni-YSZ samples after treatment in DME–CO_2. The CO_2 peak intensity of Ni-YSZ after treatment at 650 and 700 °C are very similar to those that were treated in a pure DME atmosphere at the corresponding temperatures. However, with the further increase of temperature, an obvious decrease in peak intensity was observed. As shown in Table 1, the carbon

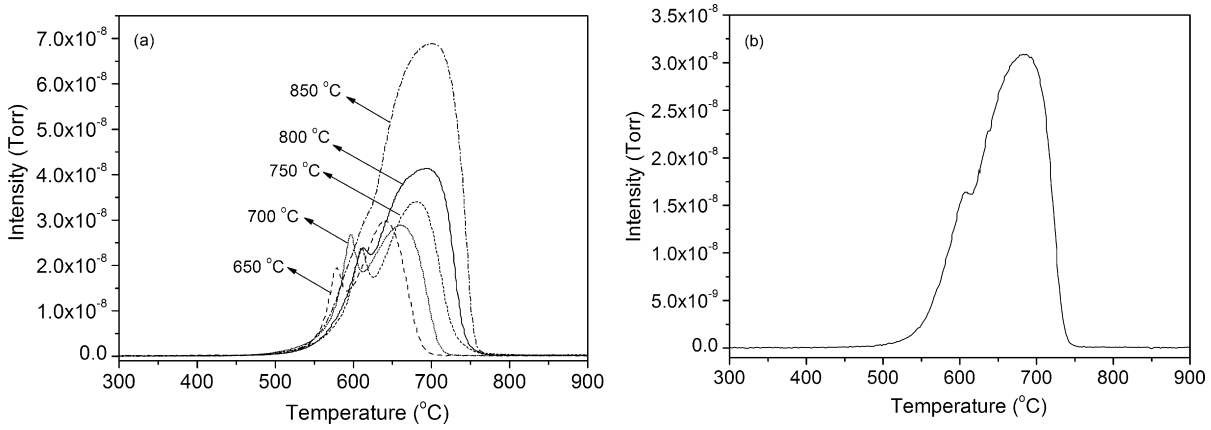

Fig. 4. O_2-TPO profiles of Ni-YSZ after treatment in pure DME for 30 min at various temperatures (a) and in pure CH_4 for 30 min at 850 °C (b).

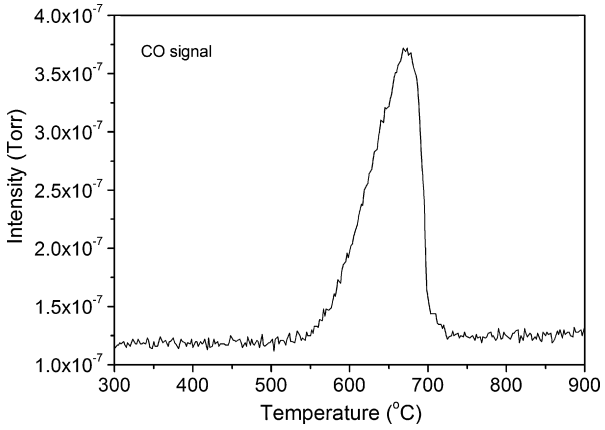

Fig. 6. CO_2-TPO profile of Ni-YSZ after treatment in pure DME for 30 min at 850 °C.

peak area is comparable for the Ni-YSZ samples after treatment in pure DME and DME–CO_2 at 650 and 700 °C. These data suggest that the introduction of CO_2 did not obviously suppress coke formation over the Ni-YSZ anode at 650 and 700 °C. However, at temperatures above 700 °C, the suppression effect of CO_2 for coke formation was clearly demonstrated; less carbon was deposited at higher operation temperatures, which is contrary to operating on pure DME. At 850 °C, the amount of carbon deposited over the Ni-YSZ that was exposed to DME–CO_2 is approximately 45 times less than when exposed to pure DME.

The suppression effect of CO_2 for coke formation over Ni-YSZ cermet is closely related to the increased O-to-C ratio. As demonstrated in the previous section, CO_2 can react with DME and methane through the formation of syngas, decreasing the coke formed from the decomposition of DME and methane. Furthermore, CO_2 may also react with the deposited solid carbon to form gaseous CO at elevated temperature, eliminating the carbon deposited over the Ni-YSZ cermet. The reactivity of deposited carbon towards CO_2 was tested by CO_2-TPR. The Ni-YSZ was first treated in an atmosphere of pure DME for 30 min at 850 °C. The obtained sample was then programmatically heated in pure CO_2. Fig. 6 shows the CO_2-TPR profile with the CO signal. The elimination of the deposited carbon by CO_2 started at ~540 °C. The negligible suppression effect of CO_2 on coke formation at 650 and 700 °C can be explained by the kinetic limitations. The rate of coke formation is likely much faster than the rate of coke gasification at such temperatures.

The structure of the deposited carbon over the various samples after treatment in DME and DME–CO_2 was investigated by the laser Raman spectroscopy. As shown in Fig. 7, two main bands are

Table 2
The value of $R\,(I_D/I_G)$ as the Raman spectral parameter of the deposited carbon over Ni-YSZ after the treatment in pure DME or DME–CO_2 at various temperatures.

Temperature (°C)	$R\,(I_D/I_G)$	
	DME atmosphere	DME–CO_2 atmosphere
850	0.39	0.53
800	0.52	0.60
750	0.70	0.84
700	1.27	1.68
650	1.45	1.78

observed in the first-order Raman spectrum of carbon materials. They are the D band (~1360 cm^{-1}) and the G band (~1580 cm^{-1}), which represent the amorphous structure and the graphite structure, respectively. The degree of structural order of the carbon can be mainly characterized by the peak integration intensity ratio in the form of $R\,(I_D/I_G)$. The value of R decreases with increasing degree of the order of the carbon [30–32], which are listed in Table 2. We find that the values of R corresponding to the deposited carbon over the Ni-YSZ decreased with increasing treating temperature in both atmospheres. The values of R are 1.45 and 0.39 after the treatment in DME at 650 °C and 850 °C, respectively. These values are 1.78 and 0.53 at the corresponding temperatures, respectively, after the treatment in DME–CO_2. The results indicate that higher treatment temperatures result in deposited carbon with higher graphite structure. Meanwhile, R values of the deposited carbon after treatment in DME–CO_2 are slightly larger than those corresponding to a DME atmosphere at the corresponding temperatures. These data imply that the degree of graphite structure of the deposited carbon is slightly reduced by introducing CO_2 into the DME atmosphere. An induced change in the coke formation mechanism by the presence of CO_2 in the reactant gases is also suggested.

The serious carbon formation by operating with DME fuel and the suppression effect of CO_2 in the fuel over real fuel cell anode under open circuit conditions were further demonstrated by the different geometric changes of the cells after the treatment in a

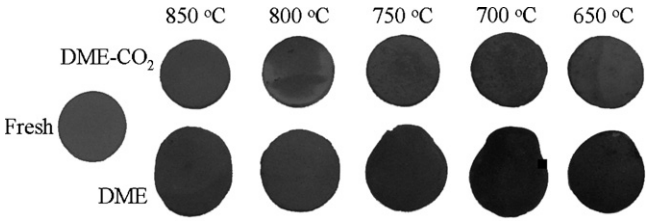

Fig. 8. Digital photos of a fresh anode and anodes after treatment in pure DME or DME–CO_2 (DME:CO_2 = 1:1) for 30 min at various temperatures.

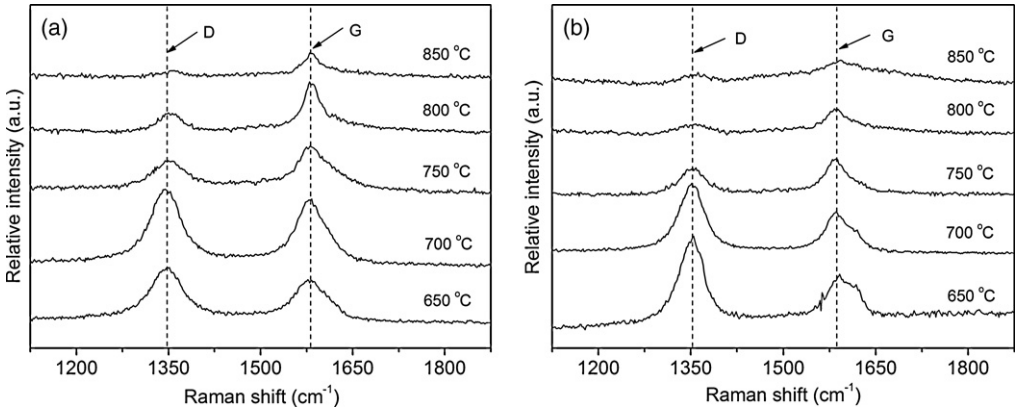

Fig. 7. Raman spectra of the deposited carbon over Ni-YSZ after treatment in pure DME (a) and DME–CO_2 (DME:CO_2 = 1:1) (b) for 30 min at various temperatures.

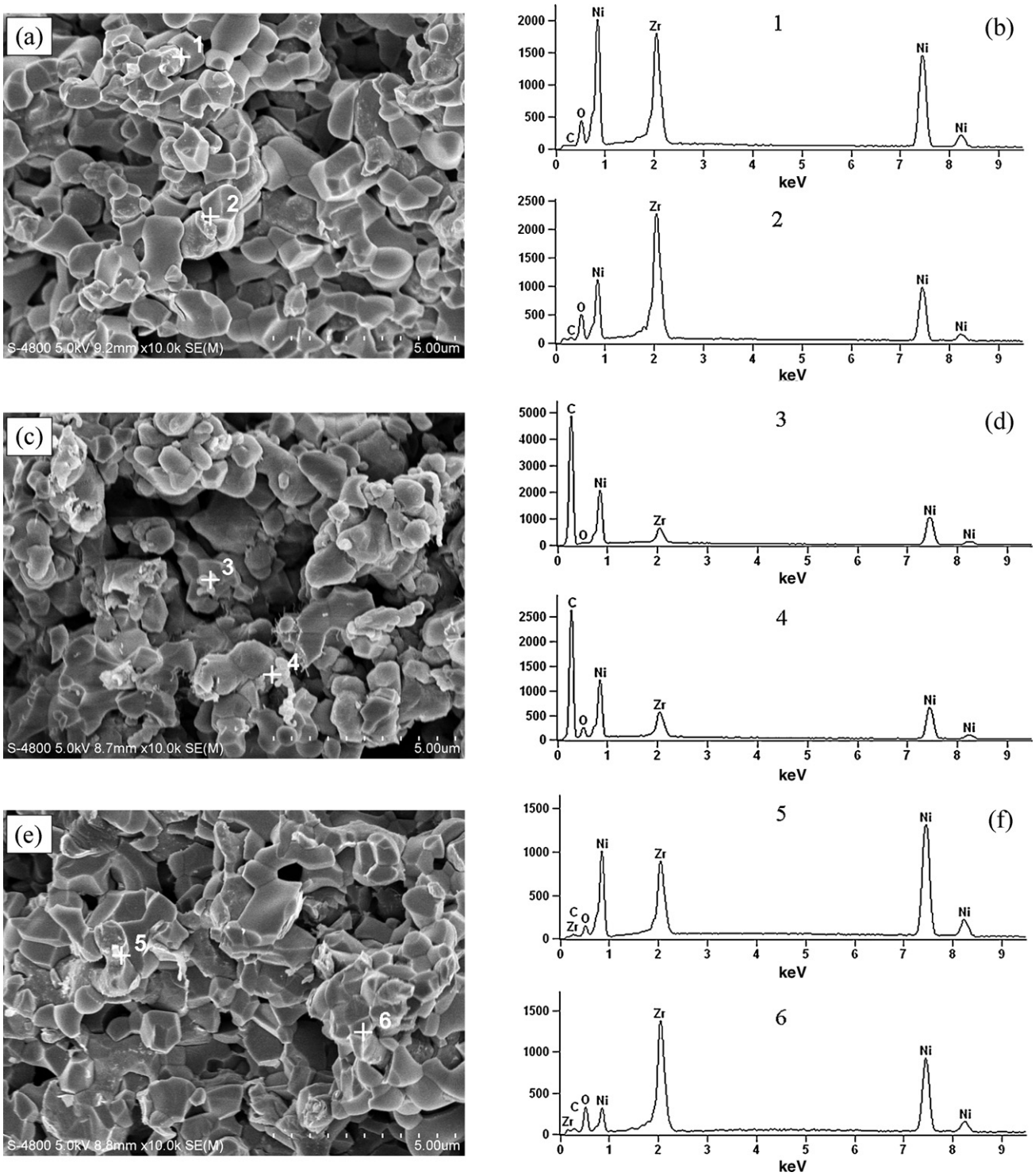

Fig. 9. SEM photos and EDX profiles of a fresh Ni-YSZ anode (a and b), after treatment in pure DME (c and d) and after treatment in DME–CO_2 (DME:CO_2 = 1:1) (e and f) under open circuit conditions at 850 °C for 30 min.

Table 3
The weight difference between the fresh cell and the cell after the treatment in pure DME or DME–CO_2 at various temperatures.

Temperature (°C)	m_f (g)[a]	m_{t1} (g)[b]	100 ($m_f - m_{t1}$)/m_f (%)	m_f (g)	m_{t2} (g)[c]	100 ($m_f - m_{t2}$)/m_f (%)
850	0.414	0.535	29.2	0.419	0.427	1.91
800	0.421	0.534	26.8	0.385	0.398	3.38
750	0.405	0.491	21.2	0.394	0.417	5.84
700	0.416	0.494	18.8	0.408	0.454	11.3
650	0.400	0.464	16.0	0.420	0.466	11.0

[a] Weight of the fresh cell.
[b] Weight of the cell after the treatment in pure DME.
[c] Weight of the cell after the treatment in DME–CO_2 gas mixtures.

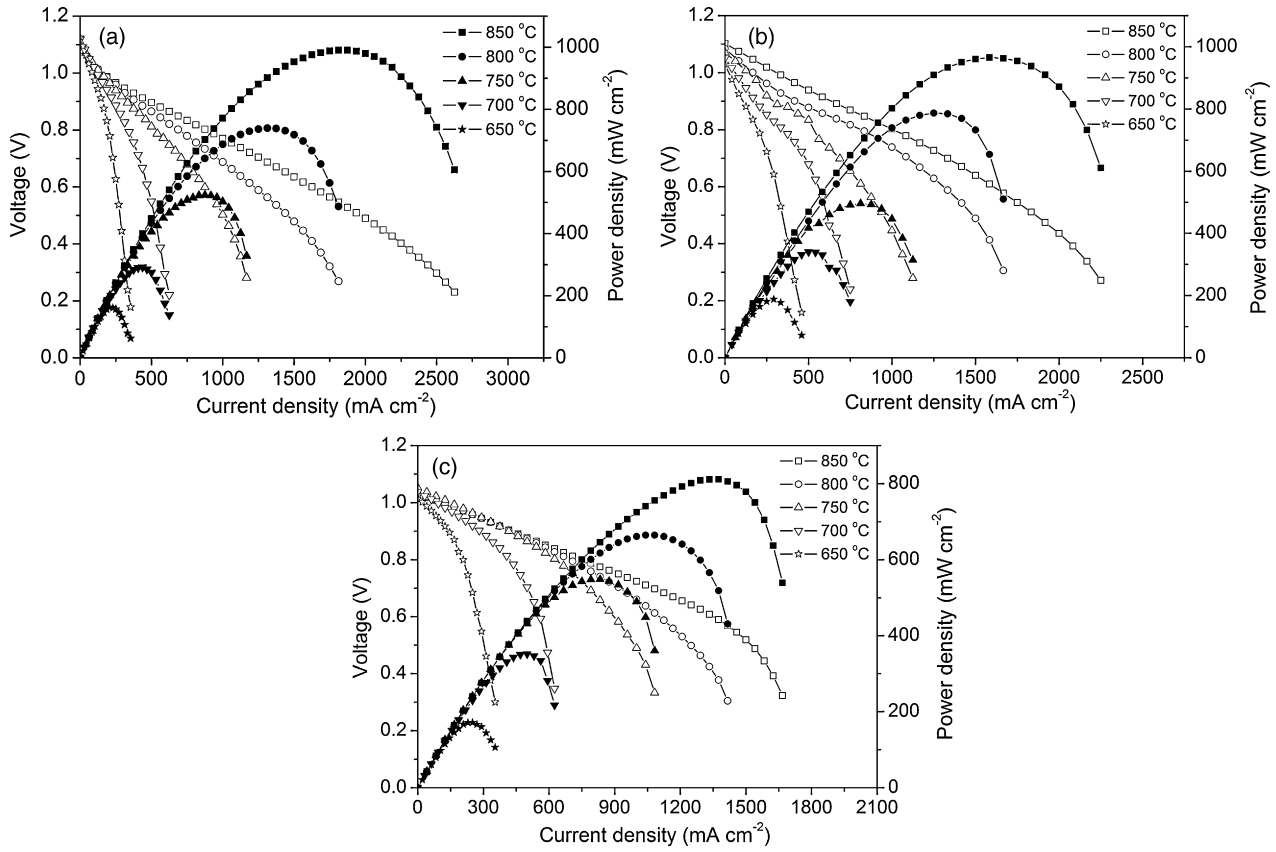

Fig. 10. The *I–V* and *I–P* polarization curves of fuel cells with Ni-YSZ anode operating on hydrogen (a), pure DME (b) and DME–CO_2 (DME:CO_2 = 1:1) (c) at various temperatures.

DME or DME–CO_2 atmosphere at various temperatures for a period of 30 min. Fig. 8 shows the digital photos of a fresh anode and anodes after treatment in pure DME or DME–CO_2 for 30 min at various temperatures. After treatment in pure DME, serious deformation of the anode disk was observed at temperatures above 650 °C; more serious deformation was observed at higher operating temperatures. Clearly, the deformation is due to coke formation over the anode. Table 3 lists the weight difference between the fresh cell and the cell after the treatment in pure DME or DME–CO_2 at various temperatures. After the treatment at 850 °C in pure DME, the weight increased approximately 29.2%. By comparison, the increase was 16.0% at 650 °C. Such weight gain is obviously from the coke formation over the anode. By introducing CO_2 into the fuel, the integrity of the cell was preserved much better. Less changes were observed in the anode geometry at higher operating temperatures. As shown in Table 3, less weight gain was also observed at elevated temperature, in good agreement with the O_2-TPO results. The presence of CO_2 effectively reduced the carbon deposition at elevated temperature, due to the reforming of DME or CH_4 by CO_2 or the elimination of deposited carbon by CO_2.

Fig. 9(a, c and e) shows SEM photos of the Ni-YSZ anode fresh, after the treatment in pure DME, and in DME–CO_2 under open circuit conditions at 850 °C for 30 min, respectively. No obvious difference between the fresh anode and the anode after the treatment in the mixture of DME–CO_2 at 850 °C for 30 min was observed. However, extra particles, which are likely the solid carbon, were observed during SEM analysis of the sample treated in pure DME. To further determine the composition of particles, the three anodes (mentioned previously) were investigated by EDX at selected positions, as shown in Fig. 9(b, d and f). We know that the samples for EDX examination were easily contaminated with carbon. Considering this effect, carbon information of the fresh anode was also obtained by EDX. As shown in Fig. 9(b), a small carbon peak was found at positions 1 and 2 of Fig. 9(a), and the average amount of carbon was 14.8 wt.%. For the sample after treatment in DME–CO_2 at 850 °C, the intensity of the carbon peaks at positions 5 and 6 of Fig. 9(e) were weak, and the average amount of carbon was 15.9 wt.%. These results indicate that there was minimal coke formation over the anode after treatment in DME–CO_2 at 850 °C. On the contrary, carbon peaks of high intensity were detected at positions 3 and 4 of Fig. 9(c) for the anode after treatment in pure DME at 850 °C. The above results agree well with the O_2-TPO results and suggest the importance of the introduction of CO_2 at proper temperatures to suppress the coke formation when operating on DME fuel.

3.3. Cell performance

Fig. 10(a–c) shows the *I–V* and *I–P* polarization curves of the anode-supported fuel cell with a conventional Ni-YSZ anode operating on 3% water humidified hydrogen, pure DME and DME–CO_2 at temperatures ranging from 850 to 650 °C. When 3% water humidified hydrogen was applied as the fuel, the peak power densities (PPDs) are 990, 739, 524, 291 and 162 mW cm^{-2} at 850, 800, 750, 700 and 650 °C, respectively; these values are 965, 786, 495, 340 and 187 mW cm^{-2} when operating on DME fuel. Similarly, by applying DME–CO_2 as the fuel, the PPDs reached 811, 664, 548, 351 and 171 mW cm^{-2} at corresponding temperatures. The results indicate that the cell power outputs are comparable when operating on hydrogen, DME fuel or DME–CO_2 gas mixtures. This outcome could be explained by the decomposition and CO_2 reforming of DME. As H_2 and CO are the main products of these reactions, similar power outputs can be obtained for the fuel cell operating on H_2, DME or DME–CO_2. In this study, the open circuit voltage (OCV) of the fuel

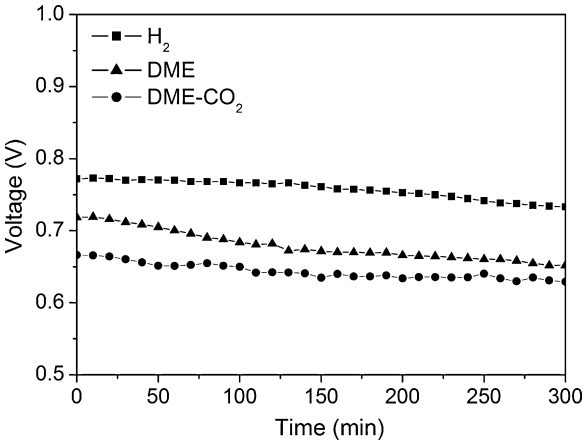

Fig. 11. Time dependence of the polarization curve of Ni-YSZ anode in different atmospheres under a constant polarization current of 1000 mA cm^{-2} at 850 °C.

cell operating on H_2 was 1.08 V at 850 °C, which is close to the theoretical value. When applying DME as the fuel, the OCV of the fuel cell was 1.10 V at 850 °C. Meanwhile, we found that the OCV decreased with decreasing operating temperatures. This behavior could be related to the nature of DME fuel. The OCV of the fuel cell operating on DME–CO_2 mixtures was 1.03 V, which was lower than pure DME. This result can be explained by the increased oxygen partial pressure in the anode chamber due to the introduction of CO_2 to pure DME.

Good operational stability is significant for practical application of fuel cells. Tests to determine the cells' stabilities when operating on DME or DME–CO_2 under a constant current density of 1000 mA cm^{-2} at 850 °C were performed. For comparison, the cell stability while operating on 3% water humidified hydrogen was also investigated under the same conditions. As shown in Fig. 11, when hydrogen was the fuel, the cell voltage remained stable at 0.77 V during the first 150 min, and slightly dropped to 0.73 V (a reduction of ~5.2%) after operation on H_2 for 300 min. By operating on pure DME fuel, the cell voltage obviously decreased with operating time, from an initial value of 0.72 V to only 0.65 V (a reduction of ~9.7%) after 300 min at 850 °C. The performance degradation can be explained by the coke formation over the anode, which covered the active sites. However, less cell degradation was demonstrated by operating on DME–CO_2. The initial value of the voltage was 0.67 V, which decreased slightly to 0.63 V (a reduction of ~5.9%) after an operational period of 300 min. Combined with the results from operating on hydrogen fuel, such degradation was unlikely due to the fuel. In other words, the cell can stably operate on DME–CO_2 at 850 °C without coke formation.

4. Conclusions

The conventional anode catalyst, Ni-YSZ, had good catalytic activity for the decomposition and CO_2 reforming of DME. When applying DEM as the fuel of SOFCs, the carbon deposition over the surface of the anode is a major concern, especially under open circuit condition. Obvious coke formation over the Ni-YSZ anode was detected in a pure DME atmosphere, and more carbon deposits were observed at higher operating temperatures. The carbon deposition can destroy the integrity of the fuel cell under OCV conditions and result in degradation of the cell's performance. Coke formation can be suppressed greatly by introducing CO_2 to the DME, especially at high temperatures. A fuel cell delivered similar power densities operating on 3% water-humidified hydrogen, pure DME and DME–CO_2, respectively. The performance of the fuel cell was stable when using DME–CO_2 as the fuel under a constant current polarization at 850 °C for 300 min, while obvious degradation was noticed when operating on pure DME. Future work will focus on modifications to the anode that will enable operation with DME fuel.

Acknowledgements

This work was supported by the National 863 Program under contract no. 2007AA05Z133, the National Basic Research Program of China under contract no. 2007CB209704, the Joint Funds of NSFC-Guangdong under contract no. U0834004, the "Outstanding Young Scholar Grant at Jiangsu Province" under contract no. 2008023, the program for New Century Excellent Talents (2008) and the Fok Ying Tung Education Foundation under contract no. 111073.

References

[1] A. Serov, C. Kwak, Appl. Catal. B 91 (2009) 1–10.
[2] M. Yano, T. Kawai, K. Okamoto, M. Nagao, M. Sano, A. Tomita, T. Hibino, J. Electrochem. Soc. 154 (2007) B865–B870.
[3] M. Cimenti, J.M. Hill, J. Power Sources 186 (2009) 377–384.
[4] S. Wasmus, A. Küver, J. Electroanal. Chem. 461 (1999) 14–31.
[5] A.L. da Silva, I.L. Müller, Int. J. Hydrogen Energy 35 (2010) 5580–5593.
[6] T.A. Semelsberger, R.L. Borup, H.L. Greene, J. Power Sources 156 (2006) 497–511.
[7] J.H. Yoo, H.G. Choi, C.H. Chung, S.M. Cho, J. Power Sources 163 (2006) 103–106.
[8] S.Z. Wang, T. Ishihara, Y. Takita, Electrochem. Solid-State Lett. 5 (2002) A177–A180.
[9] T.H. Fleisch, A. Basu, M.J. Gradassi, J.G. Masin, Stud. Surf. Sci. Catal. 107 (1997) 117–125.
[10] D. Cocco, V. Tola, J. Appl. Electrochem. 38 (2008) 955–963.
[11] J. Song, Z. Huang, X.Q. Qiao, W.L. Wang, Energy Convers. Manage. 45 (2004) 2223–2232.
[12] C. Arcoumanis, C. Bae, R. Crookes, E. Kinoshita, Fuel 87 (2008) 1014–1030.
[13] B.C.H. Steele, A. Heinzel, Nature 414 (2001) 345–352.
[14] M.M. Mench, H.M. Chance, C.Y. Wang, J. Electrochem. Soc. 151 (2004) A144–A150.
[15] I. Mizutani, Y. Liu, S. Mitsushima, K.I. Ota, N. Kamiya, J. Power Sources 156 (2006) 183–189.
[16] J.T. Müller, P.M. Urban, W.F. Hölderich, K.M. Colbow, J. Zhang, D.P. Wilkinson, J. Electrochem. Soc. 147 (2000) 4058–4060.
[17] S. Ueda, M. Eguchi, K. Uno, Y. Tsutsumi, N. Ogawa, Solid State Ionics 177 (2006) 2175–2178.
[18] J.R. Ferrell III, M.C. Kuo, A.M. Herring, J. Power Sources 195 (2010) 39–45.
[19] Y. Zhang, L.L. Lu, Y.J. Tong, M. Osawa, S. Ye, Electrochim. Acta 53 (2008) 6093–6103.
[20] G. Kerangueven, C. Coutanceau, E. Sibert, J.M. Léger, C. Lamy, J. Power Sources 157 (2006) 318–324.
[21] J.H. Yu, H.G. Choi, S.M. Cho, Electrochem. Commun. 7 (2005) 1385–1388.
[22] E.P. Murray, S.J. Harris, H.W. Jen, J. Electrochem. Soc. 149 (2002) A1127–A1131.
[23] H.X. Gu, R. Ran, W. Zhou, Z.P. Shao, J. Power Sources 172 (2007) 704–712.
[24] J.C. Ruiz-Morales, J. Canales-Vázquez, C. Savaniu, D. Marrero-López, P. Núñez, W.Z. Zhou, J.T.S. Irvine, Phys. Chem. Chem. Phys. 9 (2007) 1821–1830.
[25] E.P. Murray, T. Tsai, S.A. Barnett, Nature 400 (1999) 649–651.
[26] S.W. Tao, J.T.S. Irvine, S.M. Plint, J. Phys. Chem. B 110 (2006) 21771–21776.
[27] Y.B. Lin, Z.L. Zhan, J. Liu, S.A. Barnett, Solid State Ionics 176 (2005) 1827–1835.
[28] H.P. He, J.M. Hill, Appl. Catal. A 317 (2007) 284–292.
[29] T.J. Lee, K. Kendall, J. Power Sources 181 (2008) 195–198.
[30] A. Cuesta, P. Dhamelincourt, J. Laureyns, A. Martínez-Alonso, J.M.D. Tascón, Carbon 32 (1994) 1523–1532.
[31] M.B. Pomfret, J. Marda, G.S. Jackson, B.W. Eichhorn, A.M. Dean, R.A. Walker, J. Phys. Chem. C 112 (2008) 5232–5240.
[32] F. Tuinstra, J.L. Koenig, J. Chem. Phys. 53 (1970) 1126–1130.